Journal of Rock Mechanics and Geotechnical Engineering 9 (2017) 1112–1122

Contents lists available at ScienceDirect

Journal of Rock Mechanics and Geotechnical Engineering

journal homepage: www.rockgeotech.org

Full Length Article

Examining the effect of adverse geological conditions on jamming of a single shielded TBM in Uluabat tunnel using numerical modeling

Rohola Hasanpour [a,*], Jürgen Schmitt [b], Yilmaz Ozcelik [c], Jamal Rostami [d]

[a] Institute for Tunneling and Construction Management, Ruhr-University Bochum, Bochum, Germany
[b] Department of Civil Engineering, Darmstadt University of Applied Science, Darmstadt, Germany
[c] Department of Mining Engineering, Hacettepe University, Ankara, Turkey
[d] Department of Mining Engineering, Colorado School of Mines, Golden, USA

ARTICLE INFO

Article history:
Received 21 February 2017
Received in revised form
16 May 2017
Accepted 30 May 2017
Available online 10 November 2017

Keywords:
Single shielded tunnel boring machine (TBM)
Numerical modeling
Shield jamming
Squeezing ground
Uluabat tunnel

ABSTRACT

Severe shield jamming events have been reported during excavation of Uluabat tunnel through adverse geological conditions, which resulted in several stoppages at advancing a single shielded tunnel boring machine (TBM). To study the jamming mechanism, three-dimensional (3D) simulation of the machine and surrounding ground was implemented using the finite difference code FLAC3D. Numerical analyses were performed for three sections along the tunnel with a higher risk for entrapment due to the combination of overburden and geological conditions. The computational results including longitudinal displacement contours and ground pressure profiles around the shield allow a better understanding of ground behavior within the excavation. Furthermore, they allow realistically assessing the impact of adverse geological conditions on shield jamming. The calculated thrust forces, which are required to move the machine forward, are in good agreement with field observations and measurements. It also proves that the numerical analysis can effectively be used for evaluating the effect of adverse geological environment on TBM entrapments and can be applied to prediction of loads on the shield and pre-estimating of the required thrust force during excavation through adverse ground conditions.

1. Introduction

Despite significant progresses in the development of shielded tunnel boring machines (TBMs), the use of these machines through weak grounds and adverse geological conditions is still risky. The presence of the shield limits accesses to the tunnel walls in order to observe geological conditions and ground behaviors. Meanwhile, the excessive convergence of weak ground under high in situ stresses can impose high levels of load on the shield, which makes the machine susceptible to entrapment in weak rocks, especially under large overburden. It results in machine jamming and imposes high economic costs on tunneling companies (Farrokh and Rostami, 2008).

The complex interactions between rock mass, tunneling machine and its system components, and tunnel lining can be investigated in detail using three-dimensional (3D) numerical modeling that takes into account the main interaction parameters of ground, machine and tunnel (Cantieni and Anagnostou, 2009). Various studies have focused on computational modeling of mechanized tunneling in long and deep tunnels through adverse ground conditions. For example, Einstein and Bobet (1997), Lombardi and Panciera (1997), Graziani et al. (2007), Sterpi and Gioda (2007), Wittke et al. (2007), Ramoni and Anagnostou (2007), Amberg (2009), Schmitt (2009) and Zhao et al. (2012) conducted numerical investigations on TBM tunneling using different computational methods. Furthermore, Ramoni and Anagnostou (2010) developed dimensionless design nomograms using the results obtained from computational analyses, which allow a quick preliminary assessment of the thrust force required in order to overcome shield skin friction and avoid jamming of the shield.

Several studies were also reported in relation to the applications of computational analysis at shallow tunnels such as the numerical investigations by Finno and Clough (1985), Bernat and Cambou (1998) and Abu-Farsakh and Voyiadjis (1999) using two-dimensional (2D) approaches in their analyses. Furthermore, to

* Corresponding author.
E-mail address: ra.hasanpour@gmail.com (R. Hasanpour).
Peer review under responsibility of Institute of Rock and Soil Mechanics, Chinese Academy of Sciences.

https://doi.org/10.1016/j.jrmge.2017.05.010

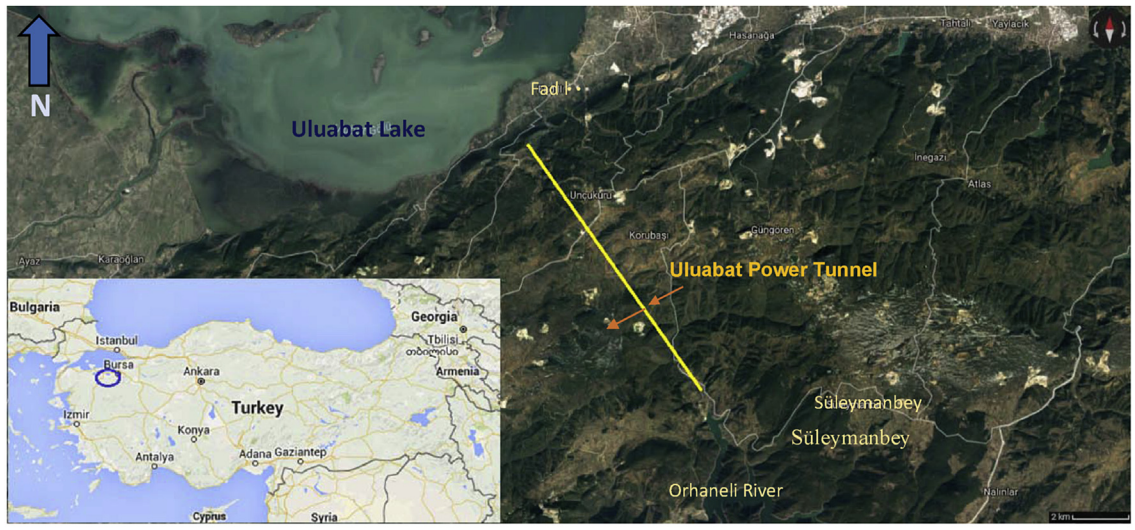

(a)

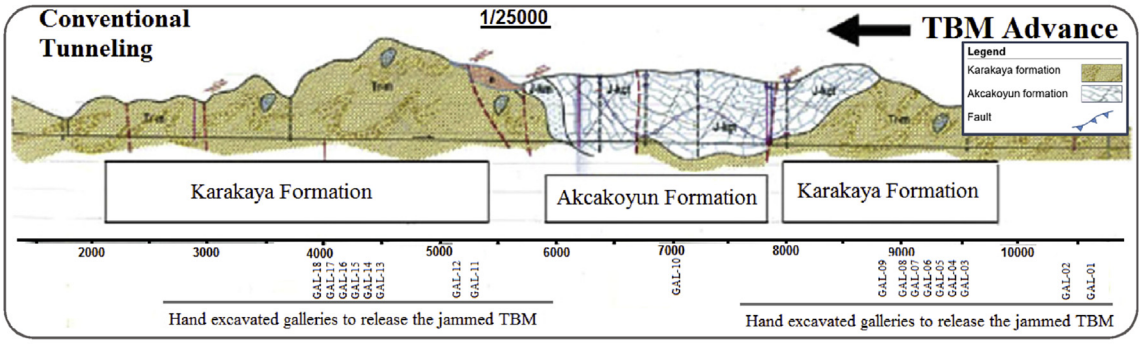

(b)

Fig. 1. (a) Project area of Uluabat power tunnel, and (b) Geological profile of Uluabat tunnel alignment and locations of hand-mined galleries to release the jammed TBM (modified from Bilgin and Algan, 2012).

examine the stress–strain behavior of the ground, advanced 3D models have been developed by Mansour (1996), van Dijk and Kaalberg (1998), Komiya et al. (1999), Dias et al. (2000) and Melis et al. (2002). Kasper and Meschke (2004, 2006a) studied the influence of TBM operational and design parameters for a shallow tunnel advance in the homogeneous, soft, cohesive soil below the groundwater table using a full 3D numerical simulation.

Results found by means of 3D finite element models have been presented by Lee and Rowe (1991), Augarde and Burd (2001) and Mroueh and Shahrour (2008). They utilized full 3D coupled-consolidation analyses for modeling of the excavation process. Moreover, the impact of gap grouting properties, cover depth and face pressure can be found in the studies by Kasper and Meschke (2006b). Recently, Chakeri et al. (2011), Hasanpour et al. (2012) and Lambrughi et al. (2012) presented a 3D numerical model using the finite difference code FLAC3D for mechanized excavations, which was capable of simulating a tunnel excavation when an earth pressure balance (EPB)-TBM was used. In addition, a full 3D modeling of tunneling using a double-shielded TBM was conducted in the studies by Hasanpour (2014) and Hasanpour et al. (2014, 2015, 2016). They considered all the main machine components and performance parameters in their numerical investigations.

In this study, 3D modeling of a single shielded TBM with EPB mode, which was used for excavation of Uluabat power tunnel through rock masses, is presented. The formations include meta-siltstone, graphitic schist, meta-claystone and metadetritics with clay matrix that exhibit squeezing behavior. The model considers the main interaction components of the machine, ground properties, performance and tunnel parameters that distinguish it from other 3D models developed for numerical simulation of shielded TBMs in the past. The model also estimates tunnel convergence during excavation and predicts the loads on the shield. The sum of applied loads on the shield can be calculated and utilized for prediction of required thrust force. The results of modeling are compared to observe the required thrust force needed to overcome frictional forces in the field for verification of the numerical outcomes.

2. Uluabat project and experienced events of shield jamming

The project area is located in the southern part of Uluabat Lake in Turkey, as shown in Fig. 1. A hydropower headrace tunnel of 11.465 km in length was excavated to transfer the water to the underground power plant. Tunnel excavation commenced in 2002 using the conventional tunneling method by applying rock bolts, shotcrete, wire-mesh and steel arches as a primary tunnel lining. However, tunneling operations were stopped in 2003 due to excessive deformations up to 1 m at tunnel walls that led to the convergence of tunnel cross-sectional area by up to 10%. It was decided that conventional tunneling was not feasible for the project due to the slow advance rates and encountered large deformations, resulting in the stoppage of tunneling operations for about two and a half years. However, a new investment company decided to continue boring the tunnel using a mixed-mode single shielded

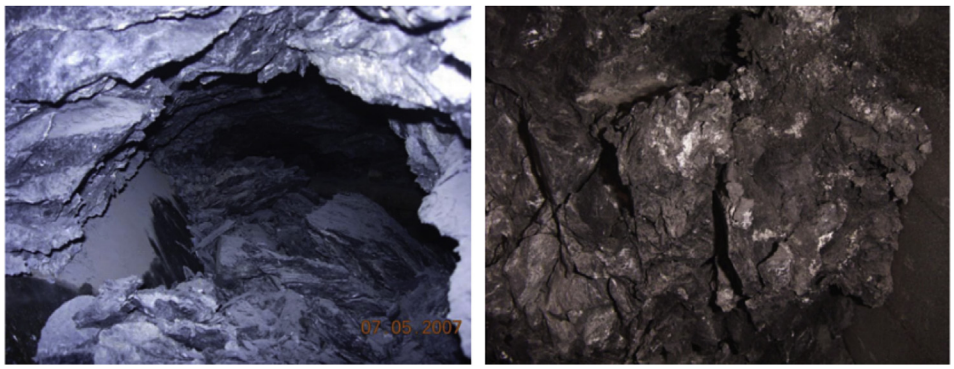

Fig. 2. General view of squeezing ground observed in the case studies from a manually excavated area (Bilgin and Algan, 2012).

TBM with a diameter of 5.05 m. The new contractor started the tunnel excavation in June 2006 and terminated it in March 2010 (Bilgin and Algan, 2012).

2.1. Encountered geological formations

Rock masses along the tunnel belong to Karakaya and Akçakoyun formations. The majority parts of tunnel alignment are situated at Karakaya formation of Triassic-aged metadetritic rocks like fine-grained meta-claystone, meta-siltstone, meta-sandstone, and graphitic schists (Fig. 2). During tunnel excavation, TBM became jammed at different places of the tunnel, frequently in metadetritic rocks due to highly squeezing characteristics of this formation. For more information about geological formations along Uluabat tunnel, readers can refer to the study by Bilgin and Algan (2012).

2.2. Description of TBM used in Uluabat tunnel

A single shielded EPB-TBM was selected for excavation of Uluabat power tunnel with general specifications listed in Table 1. An average daily advance rate of 8.6 m/d was achieved, including all stoppages such as TBM standstills and hand-mining. During tunnel excavation, the TBM became jammed 18 times at different tunnel locations and several hand-mined galleries were excavated in parallel with tunnel direction and close to the shield for releasing the entrapped machine. A total of 192 d were spent for these operations (Bilgin and Algan, 2012). In this paper, three locations with maximum overburden and maximum increase in thrust force were selected to be investigated using numerical analysis as summarized in Table 2.

3. Numerical investigations

The complex interaction between machine and surrounding rock mass should be simulated using 3D computational modeling to correctly assess the applicability of mechanized tunneling in adverse geological conditions. In this study, 3D finite difference modeling of tunneling using a single shielded TBM with EPB mode was carried out for three different areas with high squeezing behavior and large overburden, by considering TBM and ground parameters as described in Tables 3 and 4. A 3D numerical model using FLAC3D was developed for investigation of the stress–strain behavior of the rock mass in the tunnel excavated by a single shielded TBM. Calculation of the contact loading on the shield and subsequent evaluation of the required thrust force are also among the purposes.

Table 2
Locations of shield jamming with respect to related overburden and measured thrust force for each location (modified from Bilgin and Algan, 2012).

Overburden (m)	Tunnel chainage (m)	Total thrust force (MN)	Increase in thrust force during jamming of TBM (MN)
125	9400–10,400	28.6	12–17.5
250	4000–4200	28	16.5–18
300	4400–4600	28	23

Table 3
Rock mass properties along Uluabat power tunnel (Ramoni and Anagnostou, 2010; Bilgin and Algan, 2012).

Uniaxial compressive strength (MPa)	Geological strength index, *GSI*	Hoek-Brown material constant, m_i	Elastic modulus (MPa)	Bulk density (kg/m^3)
0.2–1.2	14–25	4–8	70–1000	2400–2700

Table 4
Physico-mechanical properties of machine components (Hasanpour, 2014).

Material	Elastic modulus (GPa)	Poisson's ratio	Unit weight (kN/m^3)
Shield	200	0.3	76
Segmental lining	36	0.2	30
Soft backfill	0.5	0.4	21
Hard backfill	1	0.3	24

Table 1
Characteristics of single shielded TBM used in Uluabat tunnel.

TBM diameter (m)	Maximum thrust force (kN)	Nominal torque (kN m)	Number of discs	Disc diameter (in)	Shield diameter (mm)	Shield mass (t)	Shield length (m)	TBM mass (t)	TBM length (m)	Overcut (at the crown) (cm)	Segment thickness (cm)	Concrete grade
5.05	29,000	2048 (at 6.25 rpm)	34	17	4990	69	12	335	108	4	30	C25–C30

Note: 1 in = 0.0254 m.

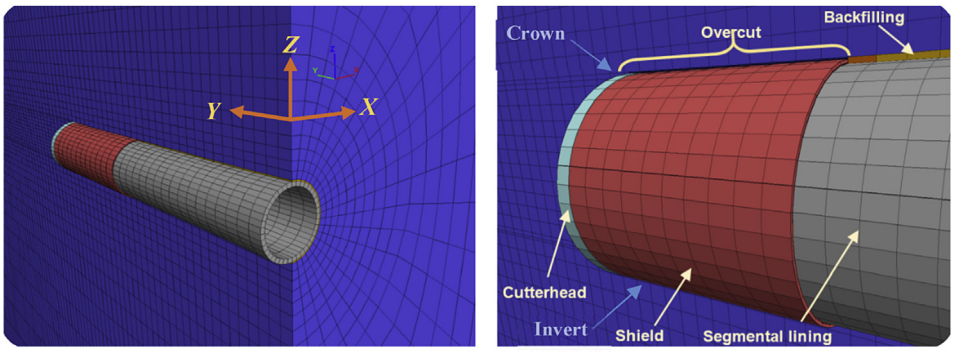

(a) (b)

Fig. 3. Screenshots of (a) numerical model and (b) discretization of the 3D model.

The rock mass was assumed to follow an elastic-perfectly plastic behavior for very weak rock mass according to Hoek-Brown failure criterion. The shield, segmental lining, and annular gap backfill were considered to behave as linear elastic materials, with pertinent properties listed in Table 3. Main features of the single shielded TBM were also considered in detail in the modeling. Application of the normal face pressure on the excavation face of the tunnel (chamber pressure) was performed in order to apply chamber pressure and thrust force to face and prevent failures at tunnel face. The developed model also considers the machine advance rate by allowing controlled relaxation of ground pressure and systematic movement of the main components of the machine. It can encounter various rock and ground conditions associated with different in situ loading situations. Another feature of the modeling is that the software used in 3D simulation allows for large strain assumptions. The non-uniform overcutting around the shield is considered successfully in the simulations. The 3D block model and discretization of the model of the single shielded TBM were selected and implemented according to rock mass and TBM characteristics, as shown in Fig. 3.

The in situ stress state is assumed to vary linearly with tunnel depth ($\sigma_v = \gamma h$). As the ratio between the horizontal and vertical stress components ($K_0 = \sigma_h/\sigma_v$) in the rock mass has been not measured, it was assumed to be 1 in this study. The contact between cutterhead and rock mass as well as that between shield and rock mass has been modeled using the interface elements on both tunnel and shield boundaries by considering non-uniform overcut between them. Normal and shear stiffness values (k_n and k_s) were

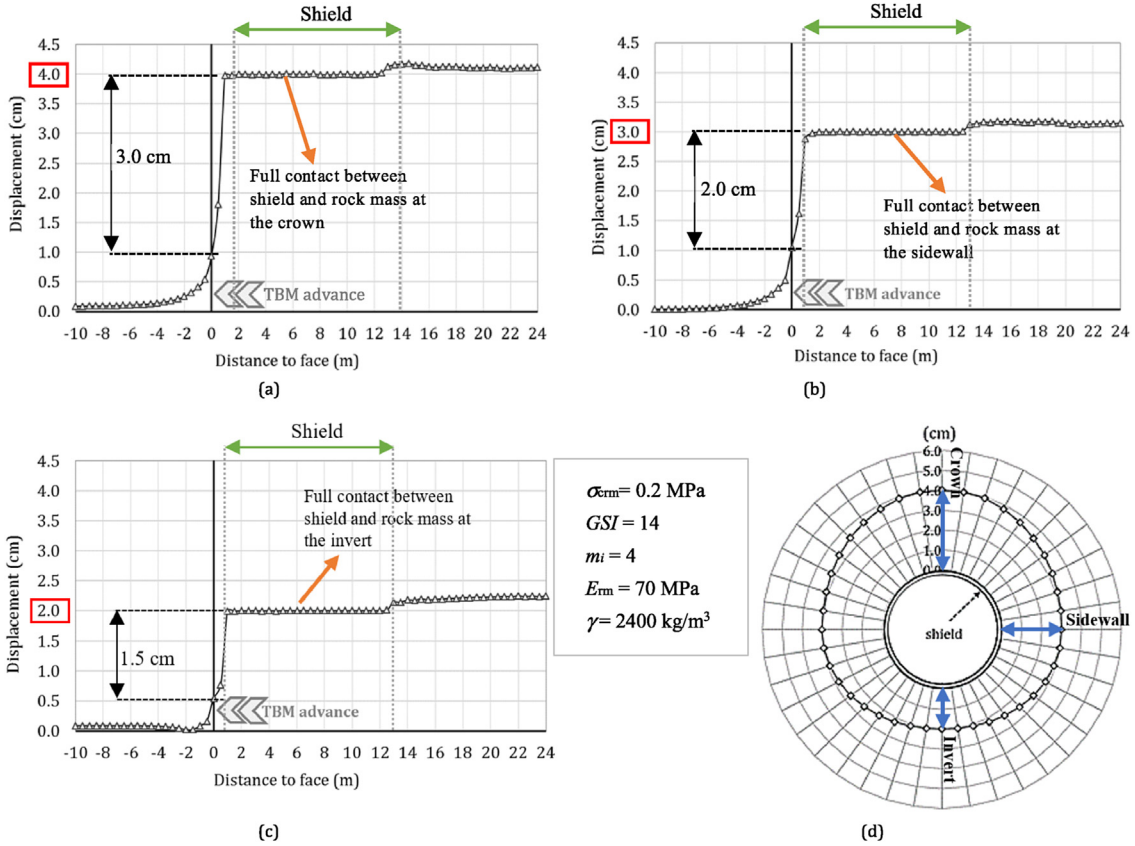

Fig. 4. (a) LDP at the crown, (b) LDP at the sidewall, (c) LDP at the invert of the tunnel, and (d) cross-sectional profile of ground deformations around shield for rock mass with the lowest strength according to Table 3.

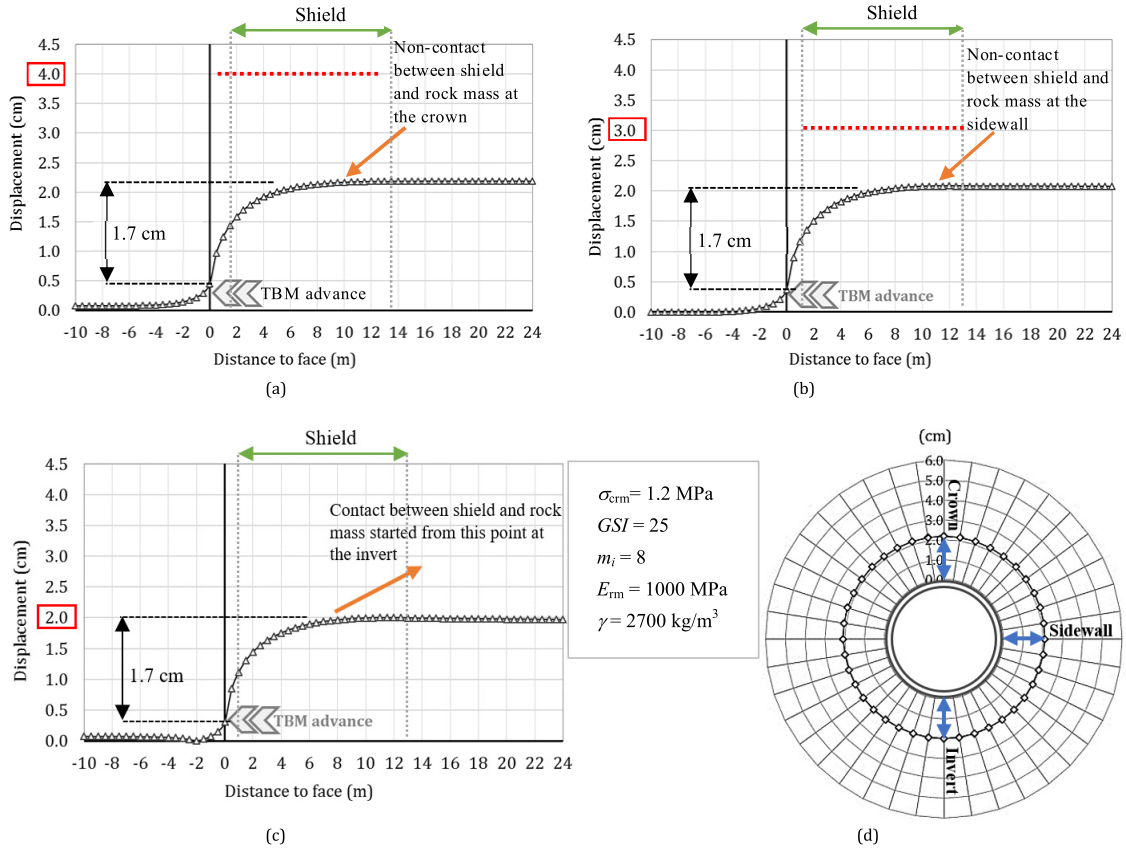

Fig. 5. (a) LDP at the crown, (b) LDP at the sidewall, (c) LDP at the invert of the tunnel, and (d) cross-sectional profile of ground deformations around shield for rock mass with the highest strength according to Table 3.

assigned to interface elements for simulating the interaction between the shield and the surrounding. k_n and k_s are assigned with a value ten times the equivalent stiffness of the softer neighboring zone, which is given by

$$k_n = k_s = \frac{K + 4/3G}{\Delta Z_{min}} \quad (1)$$

where K and G are the bulk and shear moduli of the rock mass, respectively; and ΔZ_{min} is the minimum width of an adjacent zone in the normal direction, equal to 2 cm (Itasc, 2012). k_n and k_s were calculated as 4.39×10^4 MPa/m according to the bulk and shear moduli of rock mass.

4. Computational results

Analysis results were presented for three main entrapment locations with different overburden values (125 m, 250 m, and 300 m) and changing geological conditions. Calibration and adjustment of numerical simulation were carried out based on controlled displacements at contact points between the shield and ground with respect to applied overcut. Fig. 4 depicts the cross-sectional profile of ground displacements around the shield and the longitudinal displacement profiles (LDPs) at the crown, sidewall and invert of the tunnel when the overburden is 125 m and the rock mass has the lowest strength characteristics according to Table 3. For rock mass with the highest strength properties (see Table 3), the relevant results are shown in Fig. 5.

According to Figs. 4 and 5, when the machine drives into the ground with difficult geological conditions, the ground would be in contact with the shield immediately along the entire length of the shield, and it imposes high frictional forces on the shield that may cause shield jamming and TBM stoppage (Fig. 4a–c). However, when TBM passes through the ground with relatively good conditions, the contact between the shield and the ground occurs only at the invert (Fig. 5c) and the jamming does not occur due to low frictional forces between the shield and the ground.

Since it is not practical to present results for all of the points at the tunnel circumference around the shield, to see all the trends and variations of ground pressure and shield loading, the outcomes are given as contours to reflect the results of numerical studies and simplify the understanding of loading conditions by offering visual aids. The presented contours include the longitudinal displacements in horizontal and vertical directions, maximum principal stresses and maximum shear stresses. Furthermore, ground pressure profiles around the shield for different overburden values are also given as the results of the numerical analysis.

4.1. Evaluation of shield jamming for 125 m overburden

Fig. 6a shows the contour of the maximum shear stress around the tunnel for 125 m overburden when TBM passes through the rock mass with the lowest strength (see Table 3). As can be seen in Fig. 6a, at the crown, the shear stress around the shield is minimum due to the high deformation at this point as a consequence of larger overcut. Ground pressure and hence the shear force increase at the invert because the displacement is minimum here due to minimum overcut at the invert. Furthermore, with the tunnel face advancing, shear stresses on the lining and shield rise. Fig. 6b illustrates the horizontal (Y-axis) displacement contour along the tunnel. In this

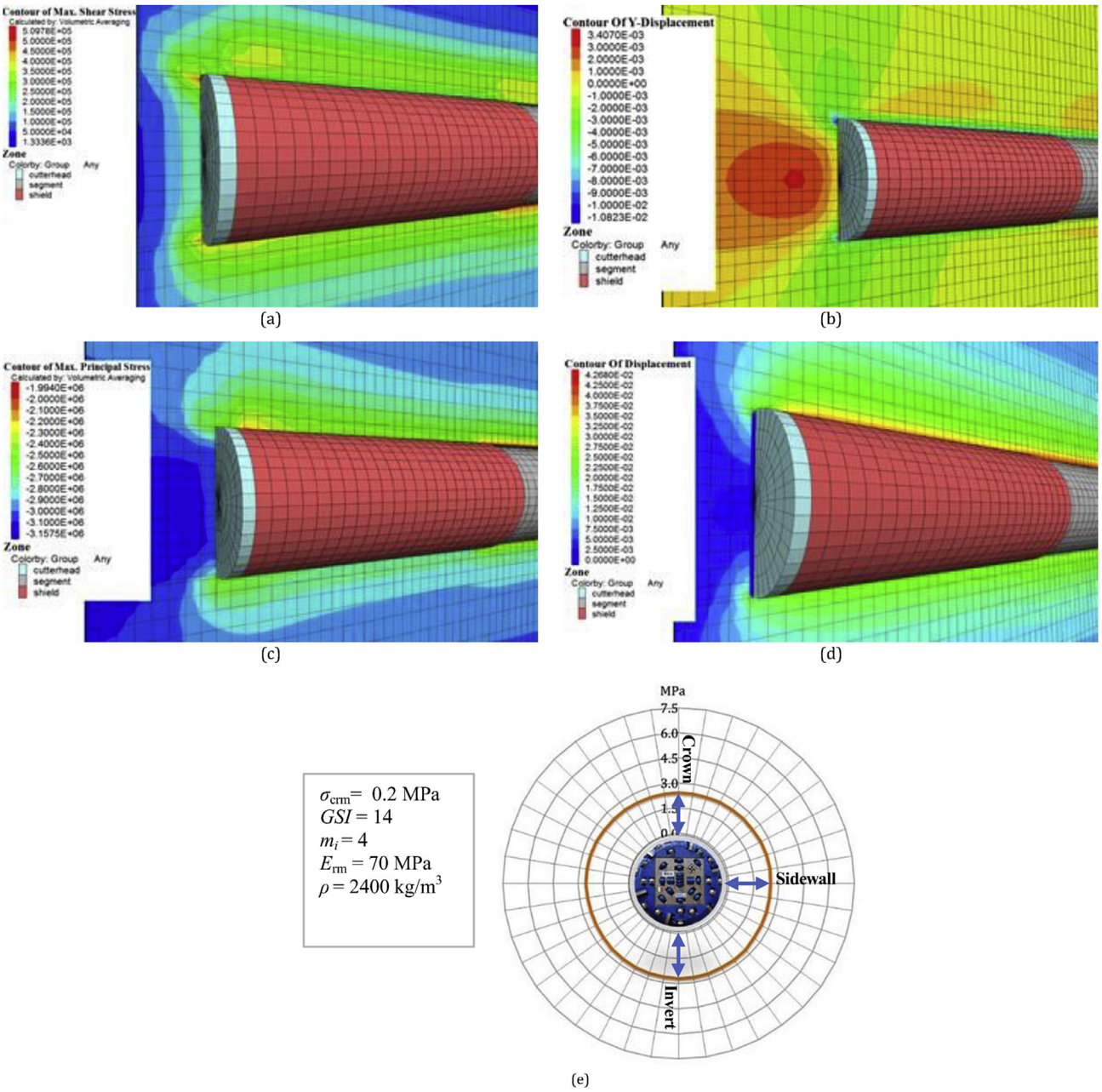

Fig. 6. (a) Contour of maximum shear stress around tunnel (unit: Pa); (b) Displacement contour around tunnel in horizontal (*Y*-axis) direction (unit: m); (c) Contour of maximum principal stress around tunnel (unit: Pa); (d) Contour of total displacement (unit: m); and (e) Distribution of average ground pressure around shield, for 125 m overburden for rock mass with the lowest strength according to Table 3.

figure, the maximum horizontal displacement (normal to the tunnel face) was calculated as about 0.34 cm at the tunnel face. This proves that the numerically applied cutterhead thrust force was calibrated to an appropriate value for stabilizing the tunnel face while excavating through squeezing rock mass.

The contours of the maximum principal stresses and total displacement around the shield and segmental linings are given in Fig. 6c and d, respectively. It can be seen that the redistribution of ground pressure around the tunnel and the related displacement circumference of the tunnel. The value of overcut is 4 cm at the crown, greater than the one at the invert (2 cm). The overcut at the tunnel invert is closed instantly after excavation and a contact occurs between the ground and the shield, then the displacement at this point remains constant and loading on the shield increases until the shield passes through the ground. Due to the larger gap at the crown, closure of overcut may occur from a certain distance to the face and cause smaller stresses on the shield.

The maximum ground pressure profile between the ground and the shield is shown in Fig. 6e. As seen in this figure, the maximum ground pressures around the shield are 2.7 MPa at the invert and 2.4 MPa at the crown. This is due to the minimum overcut at this point, which leads to immediate closure of gap and loads on the shield. Therefore, the contact pressure at this point is higher than those at other points. For calculation of the required thrust force to overcome the frictional force on the shield to propel the TBM forward, the total contact pressure over the shield is calculated. The result is then multiplied by the skin friction coefficient μ and the reduction coefficient β which is the ratio of the real shield radius r

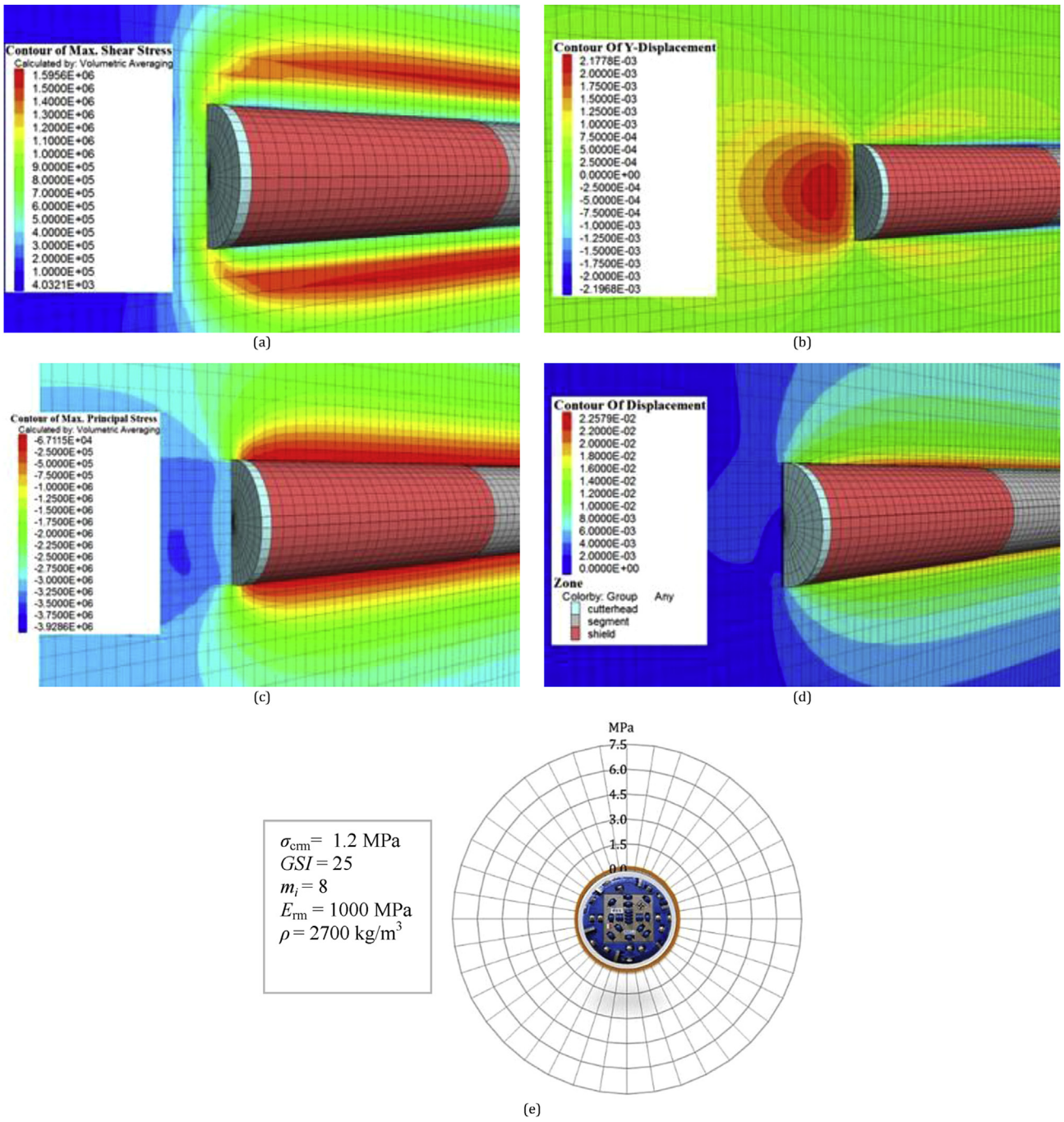

Fig. 7. (a) Contour of maximum shear stress around tunnel (unit: Pa); (b) Displacement contour around tunnel in horizontal (*Y*-axis) direction (unit: m); (c) Contour of maximum principal stress around tunnel (unit: Pa); (d) Contour of total displacement (unit: m); and (e) Distribution of average ground pressure around shield, for 125 m overburden for rock mass with the highest strength according to Table 3.

to the tunnel radius *R*. This allows for the calculation of the required maximum thrust force as can be expressed by

$$F_r = \beta\mu \sum_{i=1}^{N} P_i A_i \quad (2)$$

where *N* is the number of contact points on the shield surface area A_i (Zhao et al., 2012). The skin friction coefficient μ is assumed as 0.45 according to Gehring (1996). The required thrust force to overcome the skin friction force between the shield and the ground was calculated as 16.8 MN, and it has been measured as 17.5 MN during the TBM operation as indicated in Table 2. Hence, the required thrust force predicted using 3D numerical simulation is in a good agreement with the observed value.

The results of computational analyses for TBM-drive in relatively good geological conditions are summarized in Table 3. Fig. 7a depicts the contour of maximum shear stress where the stresses around the shield have been distributed rather uniformly around the tunnel because of the contact between the shield and the ground only at the invert of the tunnel. Fig. 7b shows the horizontal (*Y*-axis) displacement contour along the tunnel. The maximum

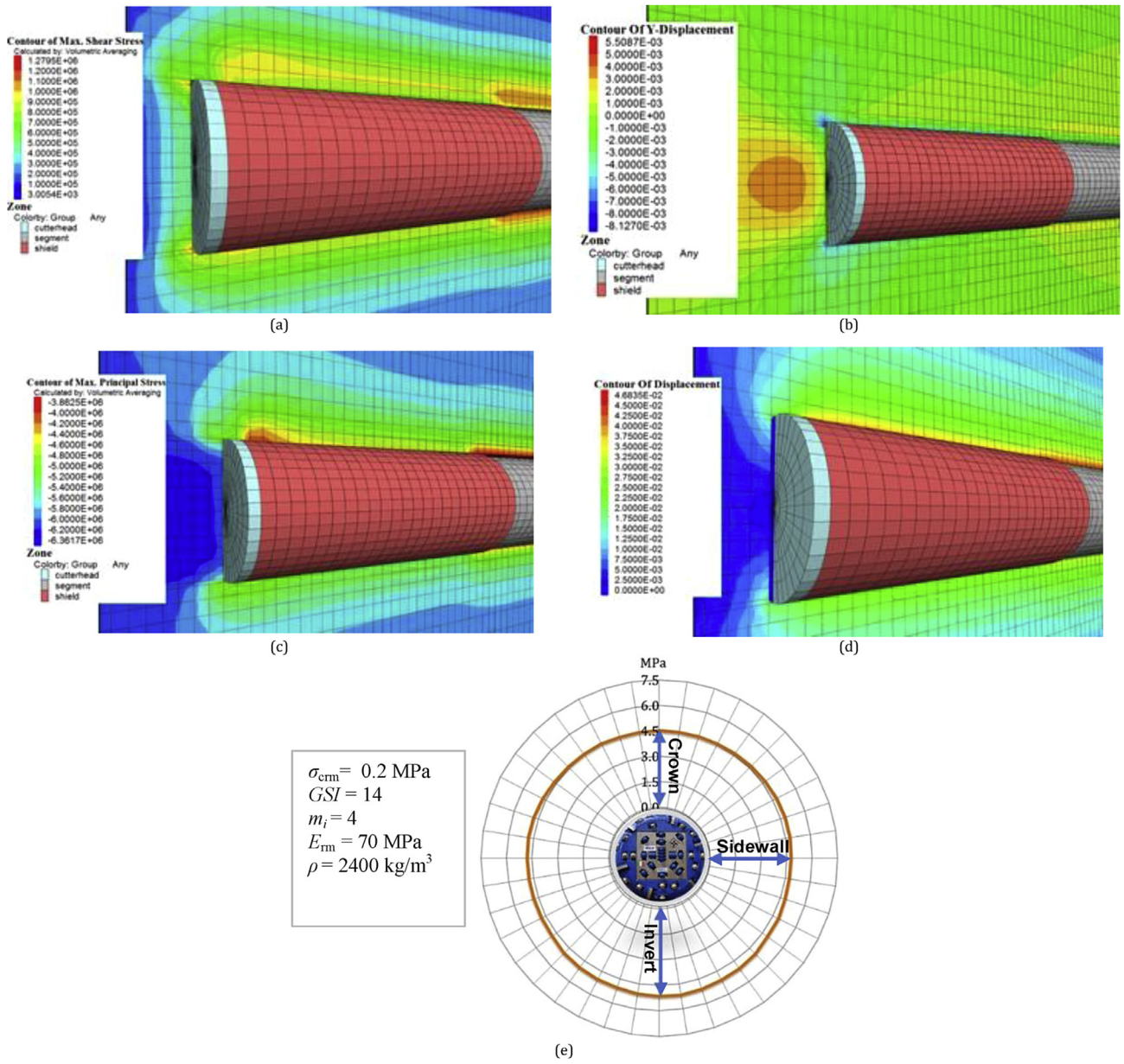

Fig. 8. (a) Contour of maximum shear stress around tunnel (unit: Pa), (b) Displacement contour around tunnel in horizontal (*Y*-axis) direction (unit: m), (c) Contour of maximum principal stress around tunnel (unit: Pa), (d) Contour of total displacement (unit: m), and (e) Distribution of average ground pressure around shield, for 250 m overburden for rock mass with the lowest strength according to Table 3.

horizontal displacement was calculated as about 0.22 cm at the tunnel face, 0.12 cm lower than the calculated value in Fig. 6b due to good ground conditions.

Fig. 7c and d illustrates the contours of maximum principal stress and total displacement around the shield and segmental linings, respectively. It can be observed that the redistribution of ground stresses and related displacements are influenced by the overcut between the shield and the ground at the invert of the tunnel because of the contact at this point. Furthermore, the closure of overcut at the crown occurs after 8 m distance to the face. In other points, stress redistributions are not affected by overcutting because the maximum ground displacements are smaller than the related overcuts at these points, and thus the overcuts at these points are not closed completely.

The profile of the applied ground pressures on the shield is depicted in Fig. 7e. The maximum contact pressures around the shield were calculated as 0.11 MPa at the invert and 0 MPa at the crown. This is because of the contact at the invert due to the weight of the shield, which causes closure of the gap and loads on the ground. The required thrust force to overcome the skin frictional force between the shield and the ground was calculated as 0.64 MN. This means that in the case of driving TBM through geological condition with the highest rock strength, the jamming of the shield does not occur. In such conditions, the thrust force is controlled by the cutter loads at the face.

4.2. Calculation of the required thrust force for 250 m overburden

Analysis results for 250 m overburden were performed in the same way as that for 125 m overburden for rock mass with adverse geological characteristics according to Table 3. The results include contours of displacements and stresses along the tunnel. Fig. 8a

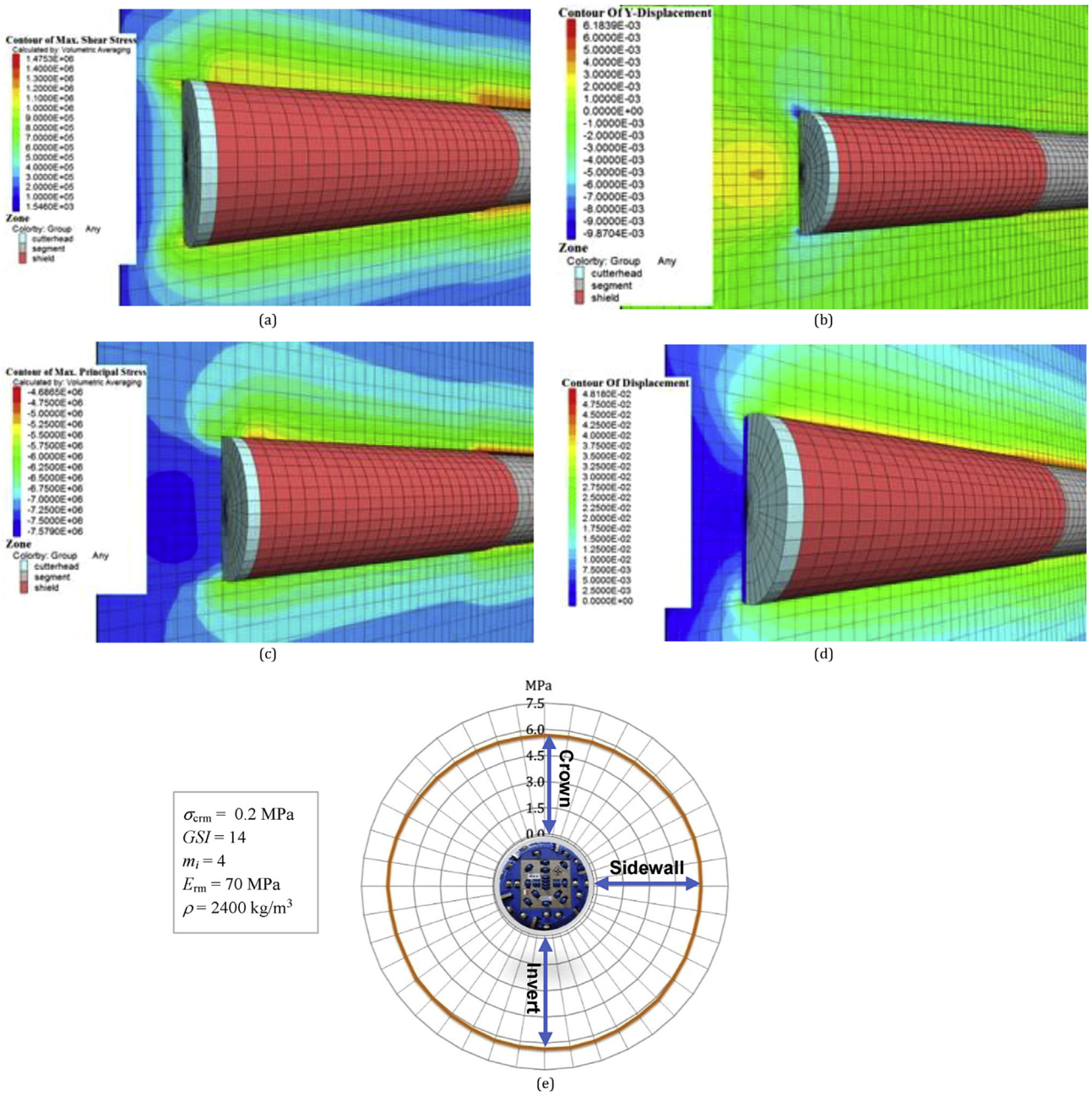

Fig. 9. (a) Contour of maximum shear stress around tunnel (unit: Pa); (b) Displacement contour around tunnel in horizontal (*Y*-axis) direction (unit: m); (c) Contour of maximum principal stress around tunnel (unit: Pa); (d) Contour of total displacement (unit: m), and (e) Distribution of average ground pressure around shield, for 300 m overburden for rock mass with the lowest strength according to Table 3.

illustrates the contour of maximum shear stresses around the tunnel for 250 m overburden. The shear stress around the shield at the crown is minimum due to the high overcut at this point, while it is increased with decreasing value of overcut at the invert. Furthermore, with the advance of the tunnel, the shear stress around the shield increases at a higher rate than that for 125 m overburden.

As shown in Fig. 8b, the maximum displacement at the tunnel face is about 0.55 cm when the thrust force applied to the tunnel face becomes in balance with the ground pressure. The contour of the maximum principal stress around the shield and linings is shown in Fig. 8c and the related displacement contour is illustrated in Fig. 8d. As shown in these figures, the displacement and the principal stress around TBM and linings are significantly influenced by the large overburden and overcut between the shield and the ground.

The maximum ground pressure profile between the ground and the shield is presented in Fig. 8e. As can be seen in the figure, due to the non-uniform overcut around the shield and smaller overcut at the invert, the maximum ground pressures of 5.15 MPa at the invert and 4.5 MPa at the crown are obtained. The required thrust force to overcome the skin friction force between the shield and the ground is calculated as 31.8 MN using numerical analysis, which is anticipated to be slightly more than the value of 28 MN recorded during tunneling operations.

In Uluabat tunnel, the thrust force could not exceed 28 MN due to the potential damage to the segmental linings. Hence, the shield was stuck and some galleries were excavated to release the

entrapped TBM. The required thrust force predicted by applying a full 3D numerical simulation proved that the required thrust force has been underestimated in the design of the project. Hence, when specifying the machine, it should be reconsidered with respect to the anticipated behavior of very weak ground under large overburden.

4.3. Jamming event at tunnel alignment with the largest overburden

Distribution of the maximum shear force around the shield, which was examined for 300 m overburden, is illustrated in Fig. 9a. As illustrated in this figure, the shear force at the crown is higher than those at other points around the shield due to the large displacement at this point. Fig. 9b illustrates the horizontal (*Y*-axis) displacement contour along the tunnel, which was calculated as about 1.5 cm at the tunnel face. The thrust force applied to the tunnel face was in balance with the ground pressure at the face. Moreover, the contour of the maximum principal stress (ground pressures) around the tunnel at contact points between the shield and the ground is illustrated in Fig. 9c, which indicates that the maximum principal stress occurs at the tunnel invert.

Given the non-uniform overcut and the minimum values at the invert, the closure of the gap between the shield and the ground occurs immediately after excavation due to the shield weight and in situ stress at this point (Fig. 9d). Therefore, the contact pressure at this point remains higher than those at other points around the tunnel. As expected, the displacement magnitudes are influenced by the non-uniform overcut between the shield and the ground (Fig. 9e). The displacement at the invert is always smaller than those at other points around the shield.

The required thrust force to overcome the skin friction force of the shield was calculated as 39.6 MN using numerical analysis, far exceeding the thrust capacity of the shield in Uluabat tunnel (28 MN). Fig. 10 summarizes the required thrust forces calculated from numerical modeling and compares them with the observed values in the field for all of the overburden scenarios. To prevent the potential damage to the segments, the maximum thrust force was limited to 28 MN. Therefore, hand-mining was necessary for some sections to release shield. The predicted values of required thrust force by applying a full 3D numerical simulation indicate that the required thrust force was not sufficient to overcome the friction force between the shield and the ground in several stretches of the tunnel, and consequently, shield entrapment occurred, causing major delays in tunneling.

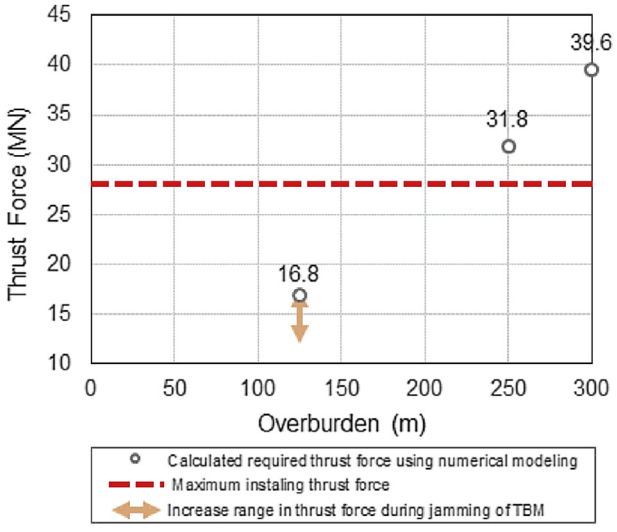

Fig. 10. Comparison of the predicted required thrust forces using 3D modeling with the observed required thrust force for all of the overburden scenarios.

5. Conclusions

This study focused on numerical modeling of the shielded TBM in Uluabat tunnel project located in Turkey to evaluate the impact of ground conditions on the loads on the shield which could increase the required thrust force to propel the shield forward. The magnitudes of the ground pressure and hence the shield thrust needed to move the machine forward were a function of the machine configuration and its interaction with the squeezing ground. To examine the interactions between the ground and the shield, 3D numerical model of the tunnel using a single shielded TBM was developed which incorporated all the geometric details of the shield as well as the true plastic behavior of the weak rock mass at the given state of in situ stresses on the ground. The developed model estimated tunnel convergence during excavation and predicted the loads on the shield. By using the results of the numerical analysis, the maximum loads applied to the shield were calculated and utilized for evaluation of the possibility of shield jamming, based on a calculation of the required thrust force.

The results indicate that the model in this study was capable of solving the complex relations between different parameters of the rock mass and shielded TBM. Moreover, 3D modeling using the finite difference model allowed for simulation of plastic deformation in the ground which is a suitable tool for the prediction of loads on the shield in the ground surrounding the tunnel. This method can be utilized in design state of the new tunnels to be excavated in the similar geological environment to evaluate the risk of shield entrapment.

The results show that the calculated loading on the shield from the numerical analysis is in an agreement with the field observation, but valid for a given set of rock mass and tunnel parameters, and the calculated values should not be generalized.

The results of this study show that the magnitudes of the loads and displacements were reasonable for given input parameters, but one should always be aware of the uncertainties regarding the geological conditions, in situ stresses, and rock mass properties when assessing the potential of shield entrapment in a given underground project.

Conflict of interest

The authors wish to confirm that there are no known conflicts of interest associated with this publication and there has been no significant financial support for this work that could have influenced its outcome.

Acknowledgements

The first author wishes to express his gratitude to Alexander von Humboldt-Foundation (AvH) for the financial support as a research fellow. The authors also gratefully acknowledge the financial support of the Scientific and Technological Research Council of Turkey (TÜBİTAK) under Project No. MAG-114M568.

References

Abu-Farsakh MY, Voyiadjis GZ. Computational model for the simulation of the shield tunneling process in cohesive soils. International Journal for Numerical and Analytical Methods in Geomechanics 1999;23(1):23–44.

Amberg F. Numerical simulations of tunnelling in soft rock under water pressure. In: ECCOMAS Thematic Conference on Computational Methods in Tunnelling, EURO: TUN 2009. Bochum, Germany: Aedificatio Publishers; 2009. p. 353–60.
Augarde CE, Burd HJ. Three-dimensional finite element analysis of lined tunnels. International Journal for Numerical and Analytical Methods in Geomechanics 2001;25(3):243–62.
Bernat S, Cambou B. Soil–structure interaction in shield tunnelling in soft soil. Computers and Geotechnics 1998;22(3–4):221–42.
Bilgin N, Algan M. The performance of a TBM in a squeezing ground at Uluabat, Turkey. Tunnelling and Underground Space Technology 2012;32:58–65.
Cantieni L, Anagnostou G. The effect of the stress path on squeezing behaviour in tunnelling. Rock Mechanics and Rock Engineering 2009;42(2):289–318.
Chakeri H, Hasanpour R, Hindistan MA, Ünver B. Analysis of interaction between tunnels in soft ground by 3D numerical modeling. Bulletin of Engineering Geology and Environment 2011;70(3):439–48.
Dias D, Kastner R, Maghazi M. Three dimensional simulation of slurry shield tunnelling. In: Kusakabe O, Fujita K, Miyazaki Y, editors. Geotechnical aspects of underground construction in soft ground. Rotterdam: A.A. Balkema; 2000. p. 351–6.
Einstein HH, Bobet A. Mechanized tunnelling in squeezing rock-from basic thoughts to continuous tunneling. In: Golser J, Hinkel WJ, Schubert W, editors. Tunnels for people, Proceedings of the 23rd ITA Assembly. Vienna, Austria: A.A. Balkema; 1997. p. 619–32.
Farrokh E, Rostami J. Correlation of tunnel convergence with TBM operational parameters and chip size in the Ghomroud tunnel, Iran. Tunnelling and Underground Space Technology 2008;23(6):700–10.
Finno RJ, Clough GW. Evaluation of soil response to EPB shield tunneling. Journal of Geotechnical Engineering 1985;111(2):155–73.
Gehring KH. Design criteria for TBM's with respect to real rock pressure. In: Tunnel boring machines – trends in design and construction of mechanized tunnelling, International Lecture Series TBM Tunnelling Trends, Hagenberg. Rotterdam: A.A. Balkema; 1996. p. 43–53.
Graziani A, Ribacchi R, Capata A. 3D-modelling of TBM excavation in squeezing rock masses. In: Brenner Basistunnel und Zulaufstrecken, Internationales Symposium BBT 2007. Innsbruck, Austria: Innsbruck University Press; 2007. p. 143–51.
Hasanpour R, Chakeri H, Özcelik Y, Denek H. Evaluation of surface settlements in the Istanbul metro in terms of analytical, numerical and direct measurements. Bulletin of Engineering Geology and Environment 2012;71(3):499–510.
Hasanpour R, Rostami J, Barla G. Impact of advance rate on entrapment risk of a double-shielded TBM in squeezing grounds. Rock Mechanics and Rock Engineering 2015;48(3):1115–30.
Hasanpour R, Rostami J, Özcelik Y. Impact of overcut on interaction between shield and ground in the tunneling with a double-shield TBM. Rock Mechanics and Rock Engineering 2016;49(5):2015–22.
Hasanpour R, Rostami J, Ünver B. 3D finite difference model for simulation of double shield TBM tunneling in squeezing grounds. Tunnelling and Underground Space Technology 2014;40:109–26.
Hasanpour R. Advance numerical simulation of tunneling by using a double shield TBM. Computers and Geotechnics 2014;57:37–52.
Itasca FLAC3D (fast Lagrangian analysis of continua in 3 dimensions) user's guide. Minneapolis, USA: Itasca Consulting Group; 2012.
Kasper T, Meschke GA. 3D finite element simulation model for TBM tunnelling in soft ground. International Journal for Numerical and Analytical Methods in Geomechanics 2004;28(14):1441–60.
Kasper T, Meschke G. A numerical study of the effect of soil and grout material properties and cover depth in shield tunnelling. Computers and Geotechnics 2006a;33(4–5):234–47.
Kasper T, Meschke G. On the influence of face pressure, grouting pressure and TBM design in soft ground tunnelling. Tunnelling and Underground Space Technology 2006b;21(2):160–71.
Komiya K, Soga K, Akagi H, Hagiwara T, Bolton MD. Finite element modelling of excavation and advancement processes of a shield tunnelling machine. Soils and Foundations 1999;39(3):37–52.
Lambrughi A, Medina Rodríguez L, Castellanza R. Development and validation of a 3D numerical model for TBM-EPB mechanised excavations. Computers and Geotechnics 2012;40:97–113.
Lee KM, Rowe RK. An analysis of three-dimensional ground movements: the Thunder Bay tunnel. Canadian Geotechnical Journal 1991;28(1):25–45.
Lombardi G, Panciera A. Problems with TBM and linings in squeezing ground. Tunnels and Tunnelling International 1997;29:54–6.
Mansour MAM. Three-dimensional numerical modelling of hydroshield tunnelling. PhD Thesis. University of Innsbruck; 1996.
Melis M, Medina L, Rodríguez JM. Prediction and analysis of subsidence induced by shield tunnelling in the Madrid metro extension. Canadian Geotechnical Journal 2002;39:1273–87.
Mroueh H, Shahrour I. A simplified 3D model for tunnel construction using tunnel boring machines. Tunnelling and Underground Space Technology 2008;23(1):38–45.
Ramoni M, Anagnostou G. Numerical analysis of the development of squeezing pressure during TBM standstills. In: Olalla C, Grossmann N, Sousa LR, editors. The Second Half Century of Rock Mechanics, 11th Congress of the International Society for Rock Mechanics (ISRM). Lisbon, London: Taylor & Francis Group; 2007. p. 963–6.
Ramoni M, Anagnostou G. Thrust force requirements for TBMs in squeezing ground. Tunnelling and Underground Space Technology 2010;25(4):433–55.
Schmitt JA. Spannungsverformungsverhalten des Gebirges beim Vortrieb mit Tunnelbohrmaschinen mit Schild. PhD Thesis. Institut für Grundbau und Bodenmechanik, Technische Universität Braunschweig; 2009 (in Germany).
Sterpi D, Gioda G. Ground pressure and convergence for TBM driven tunnels in visco-plastic rocks. In: ECCOMAS Thematic Conference on Computational Methods in Tunnelling, EURO: TUN 2007. Vienna, Austria: Vienna University of Technology; 2007. p. 89–95.
van Dijk B, Kaalberg FJ. 3D geotechnical model for the North/Southline in Amsterdam. In: Cividini A, editor. Application of numerical methods to geotechnical problems. Vienna, Austria: Springer; 1998. p. 739–50.
Wittke W, Wittke-Gattermann P, Wittke-Schmitt B. TBM-heading in rock, design of the shield mantle. In: ECCOMAS Thematic Conference on Computational Methods in Tunnelling, EURO: TUN 2007. Vienna, Austria: Vienna University of Technology; 2007. p. 98.
Zhao K, Janutolo M, Barla G. A completely 3D model for the simulation of mechanized tunnel excavation. Rock Mechanics and Rock Engineering 2012;45(4):475–97.

Dr. Rohola Hasanpour is a postdoctoral researcher in Institute for Tunneling and Construction Management at Ruhr-University Bochum. He received his PhD in Rock Mechanics and Tunneling Engineering from Hacettepe University in 2013. His PhD Thesis focused on applicability of shielded tunnel boring machines (TBMs) in squeezing ground conditions. He has published over 15 peer reviewed journal publications, more than 20 papers in international conferences and many technical reports. He worked several years as a project engineer in the field of tunneling and underground construction and is familiar with the practical aspect of rock mechanics and rock engineering. His research interests include computational modeling in geomechanics, time-dependent simulation in underground constructions and rock fracture mechanics.